UCNs

Spatiotemporal regulation ...

... of membrane channel activity in living systems has been achieved by irradiation with near-IR light ($\lambda = 808$ nm), as reported by B. Xing, G. Liu, and co-workers in their Communication on page 3031 ff. Metabolic glycan biosynthesis is used to attach lanthanide-doped upconversion nanocrystals (UCNs) to the cell surface through copper-free click cyclization. Cation influx can be controlled by irradiation and membrane-associated activities manipulated in living cells and zebrafish.

Years 150 GDCh

WILEY-VCH

Remote Regulation of Membrane Channel Activity by Site-Specific Localization of Lanthanide-Doped Upconversion Nanocrystals

Xiangzhao Ai+, Linna Lyu+, Yang Zhang, Yanxia Tang, Jing Mu, Fang Liu, Yixi Zhou, Zhenghong Zuo, Gang Liu,* and Bengang Xing*

Abstract: *The spatiotemporal regulation of light-gated ion channels is a powerful tool to study physiological pathways and develop personalized theranostic modalities. So far, most existing light-gated channels are limited by their action spectra in the ultraviolet (UV) or visible region. Simple and innovative strategies for the specific attachment of photoswitches on the cell surface without modifying or genetically encoding channel structures, and more importantly, that enable the remote activation of ion-channel functions within near-infrared (NIR) spectral window in living systems, remain a challenging concern. Herein, metabolic glycan biosynthesis is used to achieve site-specific covalent attachment of near-infrared-light-mediated lanthanide-doped upconversion nanocrystals (UCNs) to the cell surface through copper-free click cyclization. Upon irradiation with 808 nm light, the converted emission at 480 nm could activate a light-gated ion channel, channelrhodopsins-2 (ChR2), and thus remotely control the cation influx. This unique strategy provides valuable insights on the specific regulation membrane-associated activities in vivo.*

Light-gated ion channels are transmembrane protein com-

[*] X. Ai,[+] L. Lyu,[+] J. Mu, F. Liu, Prof. B. Xing
Division of Chemistry and Biological Chemistry
School of Physical & Mathematical Sciences
Nanyang Technological University
Singapore, 637371 (Singapore)
E-mail: Bengang@ntu.edu.sg

Prof. B. Xing
Institute of Materials Research & Engineering (IMRE)
Agency for Science, Technology and Research (A*Star)
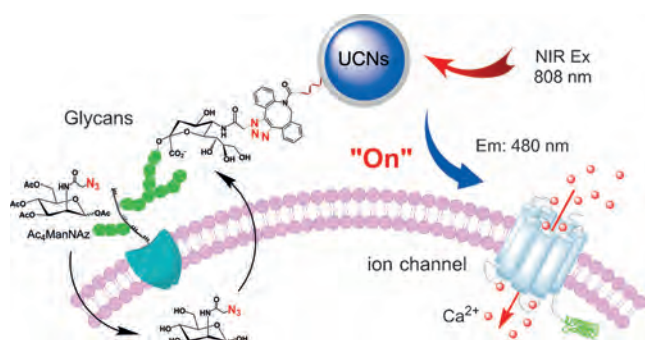Singapore 117602 (Singapore)

Dr. Y. Tang
Lee Kong Chian School of Medicine
Nanyang Technological University
Singapore, 637371 (Singapore)

Y. Zhou, Prof. Z. Zuo
State Key Laboratory of Cellular Stress Biology
School of Life Sciences, Xiamen University
Xiamen, Fujian, 361005 (China)

Y. Zhang, Prof. G. Liu
State Key Laboratory of Molecular Vaccinology and Molecular Diagnostics, Center for Molecular Imaging and Translational Medicine, School of Public Health
Xiamen University, Xiamen, Fujian, 361005 (China)
E-mail: gangliu.cmitm@xmu.edu.cn

[+] These authors contributed equally to this work.

Supporting information and the ORCID identification number(s) for the author(s) of this article can be found under:
http://dx.doi.org/10.1002/anie.201612142.

plexes that can spatially and temporally regulate cellular activities through optical control of the movement of ions across the cell membrane. They have been identified as valuable tools to explore basic physiological processes on the cellular level and to facilitate the development of therapeutic agents for disease treatment.[1] By right, several naturally occurring light-dependent regulatory proteins have been converted into genetically encoded light-sensitive effectors for the specific manipulation of cell signaling and gene expression in various types of cells and tissues. In addition to utilizing natural photoreceptor proteins, alternative light-gated channel systems have also been constructed by chemical modification or mutagenesis of photoswitchable ligands on channel structures in order to modulate cell functions with spatiotemporal precision.[2] Currently, most of the established light-gated channels are mainly activated by UV or visible light, which may raise concerns regarding photodamage and limited light penetration, as well as inherent absorption and scattering caused by endogenous chromophores including hemoglobin, flavins, and melanin.[3] Although two-photon optogenetic stimulation has been suggested to overcome these obstacles in part, such long-wavelength excitation usually requires complex experimental setups and there is limited conductivity for light-sensitive channels arising from narrow absorption cross-sections.[4] Recently, some initial studies demonstrated the possibility of lanthanide-doped upconversion nanocrystals (UCNs) to enable the activation of channel functions with excitation at 980 nm,[5] mainly due to their unique capability to convert tissue-penetrable near-infrared (NIR) light irradiation into UV or visible emissions.[6] Despite successful attempts, in principle the manipulation of cellular activities requires genetically engineering UCNs onto membrane channel structures,[5a] or the activation can be realized by randomly mixing hybrid UCN scaffolds within targeted cells.[5b–e] Simple and rational design that allows specific localization of photoswitchable platforms on the cell surface without altering channel proteins, and more importantly, the precise regulation of ion-channel activities under both in vitro and in vivo conditions via a more secure and effective light source at the NIR window remains a technical challenge.

Herein, we present a simple and unique approach based on native metabolic glycol-biosynthesis pathways to covalently localize NIR (808 nm)-light-responsive UCNs on the cell surface to achieve accurate manipulation of the light-gated channel activities in living cells and animals. As shown in Scheme 1, through an intrinsic metabolic process, we incorporate a monosaccharide precursor, peracetylated N-azidoacetylmannosamine (Ac4ManNAz) functionalized with

Scheme 1. Metabolic labeling strategy for site-specific covalent localization of NIR-light-responsive UCNs on the cell membrane to achieve precise regulation of ion channel function.
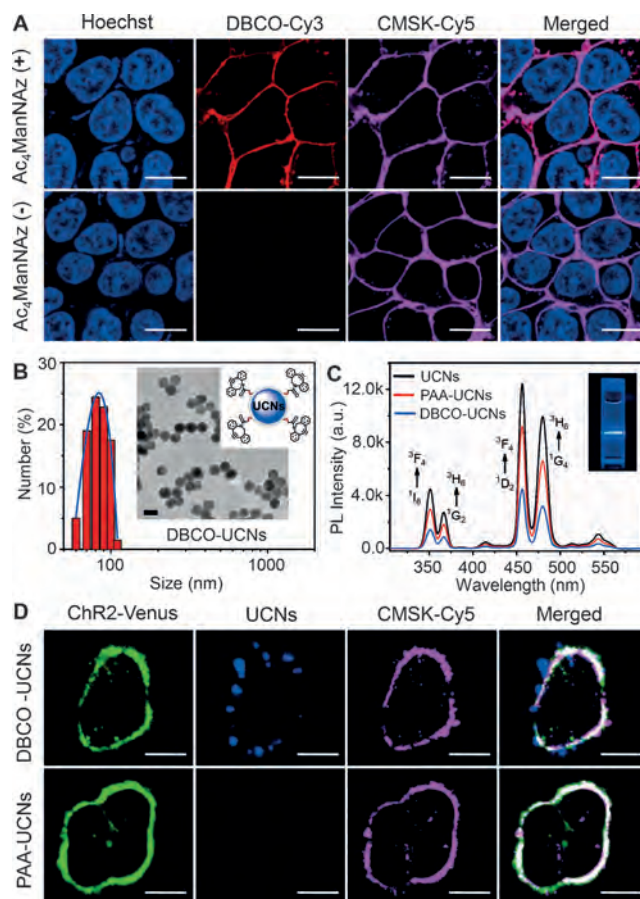

Figure 1. Characterization of azido groups and site-specific covalent localization of UCNs on the cell membrane. A) Imaging azido groups on the membrane of HEK293 cells stained with DBCO-Cy3 (10 μM) after feeding with (top) or without (bottom) $Ac_4ManNAz$ (50 μM). Blue: Hoechst 33342 (E_x: 405 nm, E_m: 460/50 nm), red: DBCO-Cy3 (E_x: 543 nm, E_m: 580/50 nm), violet: CMSK-Cy5 (E_x: 633 nm, E_m: 670/50 nm). Scale bar: 20 μm. B) TEM and DLS results of DBCO-UCNs, scale bar: 50 nm. C) Upconversion emissions of UCNs, PAA-UCNs, and DBCO-UCNs (1 mg mL^{-1}) under 808 nm excitation. Inset: luminescence photograph of UCNs with 808 nm irradiation. D) Confocal imaging of azido-expressed HEK293 cells incubated with DBCO-UCNs (top) and PAA-UCNs (bottom) for 2 h at 100 μg mL^{-1}. Green: ChR2-Venus (E_x: 488 nm, E_m: 530/50 nm), blue: UCNs (E_x: 543 nm, E_m: 580/50 nm), violet: CMSK-Cy5 (E_x: 633 nm, E_m: 670/50 nm). Scale bar: 10 μm.

a bioorthogonal azido tag, into glycoconjugates (e.g. sialic acids etc) on the cell membrane.[7] NIR-light-sensitive UCNs doped with neodymium (Nd^{3+}) ions that can respond to 808 nm laser excitation were attached to the tag through a modified dibenzyl cyclooctyne (DBCO) moiety. At this spectral window, UCNs are known to display minimized water absorption and overheating effects as compared to UCNs irradiated at 980 nm.[8] Based on successive copper-free click reactions, the UCN conjugates could be site-specifically anchored onto the plasma membrane.[9] Upon 808 nm light illumination, the upconverted emission at 480 nm from UCNs could activate the light-gated channelrhodopsins-2 proteins (ChR2),[10] and therefore manipulate cation influx (e.g., Ca^{2+}) across the cell membrane to remotely regulate physiological processes under living conditions.

First, we started the covalent glycan labeling approach by incorporation of azido groups into the living cell membrane via native metabolic biosynthesis. Basically, the N_3-tagged glycans could be introduced to human embryonic kidney 293 (HEK293) cells through intrinsic metabolism by simply feeding the $Ac_4ManNAz$ precursor. A copper-free click reaction based on the DBCO-conjugated fluorophore (e.g. DBCO-Cy3) as a bioorthogonal linkage was then performed in $Ac_4ManNAz$-treated HEK293 cells. The covalent labeling of the cell surface was monitored by confocal microscopy and flow cytometry (FCM) analysis. As shown in Figure 1 A, after feeding the cells with $Ac_4ManNAz$ (50 μM), the bright red fluorescence from Cy3 was visualized on the HEK293 cell membrane. Moreover, similar cell-surface staining was also confirmed by a standard membrane tracker, CMSK-Cy5 (Figure 1 A).[11] In control experiments no significant signal was detected in the cells that had not been incubated with $Ac_4ManNAz$ or in the cells that had been pretreated with reagent (e.g. DBCO-NH_2) to block the N_3 groups on the cell surface (Figures S1 and S2), suggesting the high feasibility of the covalent conjugation of functional moieties on the membrane through the native metabolic biosynthetic pathways.

Furthermore, in order to achieve precise regulation of membrane channel activities, a light-gated ion-channel protein, ChR2, was engineered on the cell surface to mediate the influx of essential signaling ions (e.g. Ca^{2+}) in the cytoplasm. The successful expression of ChR2 on the membrane was

confirmed by the presence of the green fluorescent protein (GFP) marker (Venus) using confocal microscopy (Figure 1 D and Figure S3). Moreover, to conduct NIR-light-mediated regulation of ion-channel functions, UCNs doped with Nd^{3+} ions were used as novel transducers owing to their promising light-converting property at 808 nm. Basically, the Nd^{3+}-doped UCNs were functionalized with polyacrylic acid (PAA) to improve their dispersion stability in buffer and to facilitate subsequent chemical modification (Figure S4). In order to covalently anchor UCNs on the azido-tagged cell surface, DBCO moieties were coupled with a carboxyl group in PAA to afford DBCO-UCNs (Figure S4). The fluorescent conjugation through 5-carboxyfluorescein-azide (FAM-N_3) confirmed the effective coating of DBCO on the UCNs surface

and the optimal amount of DBCO on the UCNs surface was determined as ca. 320 nmol mg^{-1} (Figure S5). Transmission electron microscopy (TEM) revealed the spherical morphology of core–shell DBCO-UCNs particles with an average diameter of roughly 40 nm (Figure 1 B and Figure S6). Meanwhile, the hydrodynamic diameter in buffer solution was also determined as 96.4 ± 10.4 nm on the basis of dynamic light scattering (DLS) analysis (Figure 1 B). The DBCO-UCNs particles displayed strong luminescence at 456 nm and 480 nm upon light excitation at 808 nm (Figure 1 C), which matched well with the maximum absorption of ChR2 at 480 nm.[10] Finally, the subsequent copper-free click cyclization enabled the effective linkage of DBCO-UCNs onto the N$_3$-tagged HEK293 cell membrane. As shown in Figure 1 D, the UCNs were obviously visualized on cell surface (blue) after 2 h incubation, and exhibited similar membrane staining with ChR2-Venus (green) and the standard membrane tracker (CMSK-Cy5, red). Furthermore, there were negligible signals observed in control studies when the N$_3$-tagged cells were incubated with DBCO-free UCNs (PAA-UCNs), or when the cells without N$_3$ groups on surface were treated with DBCO-UCNs (Figure 1 D, Figures S7 and S8). These results clearly indicated the metabolic glyco-biosynthesis can site-specifically localize DBCO-UCNs on living cell membranes through the copper-free bioorthogonal click reaction.

To further investigate the possibility of NIR-light-responsive UCNs for remote manipulation of membrane channel activities, 808 nm light was utilized to irradiate the covalently localized UCNs transducers on the cell surface. The upconverted blue emission was used to activate the light-gated ChR2 channels to facilitate the Ca^{2+} ion influx across the membrane. The level of intracellular Ca^{2+} ions was measured through a standard fluorescent Ca^{2+} indicator, Rhod-3 AM.[12] As shown in Figure 2 A, 808 nm light irradiation of DBCO-UCNs-labeled HEK293 cells with ChR2 expression could lead to a significant increase of red fluorescence in the cytosol, while no apparent fluorescence increment was recorded in control experiments for either N$_3$-tagged cells treated with DBCO-free UCNs, or N$_3$-absent cells incubated with DBCO-UCNs (Figure S9). Moreover, the quantitative FCM analysis also showed that such NIR-light-responsive fluorescence enhancement was light-dose-dependent, clearly suggesting that the intracellular Ca^{2+} influx could be precisely regulated by the DBCO-UCNs located on the membrane upon NIR-light irradiation (Figure 2 B). We also carried out standard whole-cell patch-clamping studies to measure the NIR-light-mediated ionic photocurrent flow across the membrane.[2b, 10] As indicated in Figure 2 C, after 808 nm light illumination, a remarkable inward photocurrent response was immediately observed (ca. 280 pA) in the DBCO-UCNs-labeled HEK293 cells with ChR2 expression, which was similar to the results obtained upon illumination at 480 nm. Meanwhile, there were no significant signals observed in the ChR2-expressing HEK293 cells without DBCO-UCNs labeling and the ChR2-absent cells treated with DBCO-UCNs (Figure 2 C).

Moreover, as a ubiquitous intracellular messenger, Ca^{2+} ions play significant roles in many physiological processes including cell proliferation, differentiation, and apoptosis.[13]
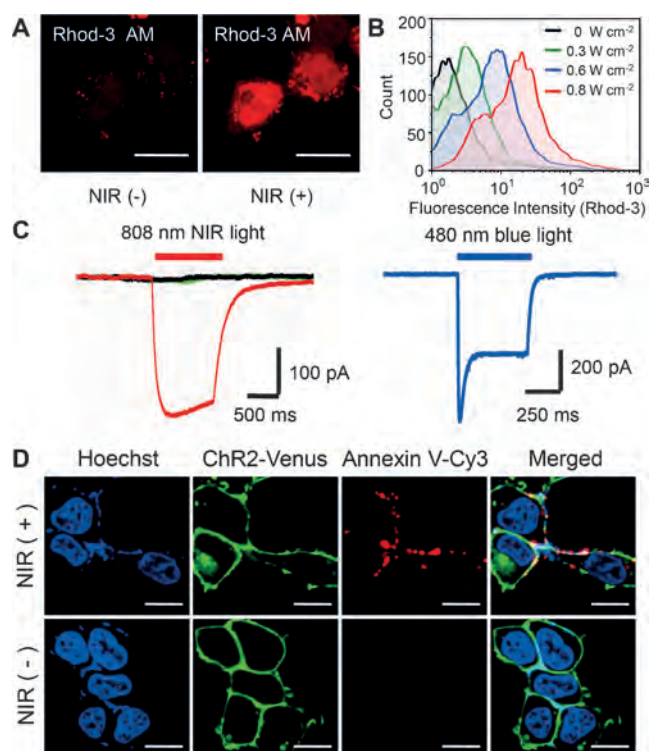

Figure 2. Regulation of cell activities upon 808 nm light illumination. A) Cellular Ca^{2+} imaging using Rhod-3 AM before and after NIR-light irradiation (0.8 W cm^{-2} for 20 min). E_x: 561 nm, E_m: 610/75 nm. B) FCM analysis of cellular Ca^{2+} with different light dosages. C) Photocurrents in ChR2-expressing HEK293 cells incubated with DBCO-UCNs for 2 h under 808 nm (red) and 480 nm (blue) excitation. ChR2-expressing cells only (black) and UCNs-labeled cells without ChR2 expression (green) were used as controls. D) Live-cell apoptosis imaging after DBCO-UCNs (100 µg mL^{-1}) incubation with (top) and without (bottom) 808 nm light irradiation (0.8 W cm^{-2} for 40 min). Blue: Hoechst 33 342 (E_x: 405 nm, E_m: 460/50 nm), green: ChR2-Venus (E_x: 488 nm, E_m: 530/50 nm), red: Annexin V-Cy3 (E_x: 543 nm, E_m: 580/50 nm). Scale bar: 20 µm.

To this direction, we examined the ability of cell-surface-localized DBCO-UCNs to mediate Ca^{2+}-dependent apoptosis upon their illumination at 808 nm. Typically, Cy3-tagged Annexin V was applied as an indicator to study the apoptosis in HEK293 cells. As shown in Figure 2 D, the DBCO-UCNs-labeled cells presented an obvious red fluorescence on the cell membrane after 808 nm light excitation. In control experiments, there was no significant fluorescence in cells treated with DBCO-free UCNs under irradiation at 808 nm, and in the cells incubated with DBCO-UCNs but without NIR light illumination (Figure 2 D and Figure S10). Similar NIR-light-responsive fluorescence enhancement was also obtained through FCM analysis (Figures S11 and S12), which confirmed the occurrence of apoptosis with 808 nm light irradiation of DBCO-UCNs localized on cell membrane. These results unequivocally indicated that cell-surface-localized UCNs could serve as a unique photoswitch to precisely regulate cation movement for the specific manipulation of cellular functions.

Furthermore, we also exploited the in vivo metabolic glycan labeling in zebrafish, one commonly used animal

model for human disease screening and sophisticated imaging studies.[14] Typically, we implanted N₃-tagged HEK293 cells with ChR2 expression into the yolk sac of zebrafish larvae at 48 hours post-fertilization (hpf). The bright green fluorescence in the larvae abdomen indicated the successful implantation of cells in zebrafish (Figure 3 and Figure S13). To study
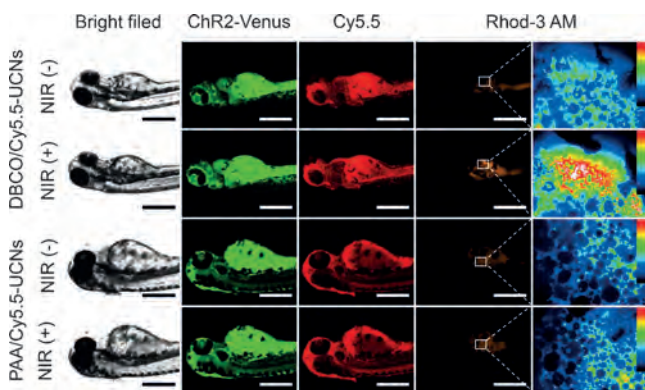

Figure 3. In vivo fluorescence imaging with and without NIR light treatment (0.8 Wcm⁻² for 2 h) in zebrafish incubated with DBCO/Cy5.5-UCNs and PAA/Cy5.5-UCNs ($n = 20$). The Ca^{2+} response in fish was monitored by Rhod-3 AM and analyzed with pseudo-colored imaging. Green: ChR2-Venus (E_x: 488 nm, E_m: 530/50 nm), red: Cy5.5 (E_x: 635 nm, E_m: 680/30 nm), yellow and pseudo-color: Rhod-3 AM (E_x: 561 nm, E_m: 610/75 nm). Scale bar: 400 μm.

the feasibility of the metabolic glycan labeling for localized UCNs attachment in vivo, the larvae were further incubated with DBCO/Cy5.5-UCNs for 12 h, which enabled the effective click linkage of UCNs onto the N₃-tagged cells in the abdominal cavity of the larvae ($n = 20$). Moreover, an NIR dye, Cy5.5, was coated on the UCNs surface to monitor the localization of particles in vivo. The systematic imaging studies indicated the bright fluorescence at 0 hour post-incubation (hpi), suggesting the effective uptake of UCNs in larvae (Figure S14). Upon 72 h clearance, the obvious fluorescence in zebrafish incubated with DBCO/Cy5.5-UCNs could be still observed, while only a very weak signal was detected in fish treated with the control PAA/Cy5.5-UCNs without DBCO on the surface. Similarly, the effective cellular uptake was also confirmed by inductively coupled plasma (ICP) analysis; a higher Y^{3+} ion distribution in zebrafish with the incubation of DBCO/Cy5.5-UCNs was found at 72 hpi (Figure S15), clearly indicating that the metabolic glycan labeling could greatly enhance the efficiency of UCNs accumulation under in vivo conditions.

More significantly, in order to remotely regulate the membrane channel activities in vivo, we utilized 808 nm NIR light to irradiate the larvae and monitored the cation influx in zebrafish ($n = 20$) by using a Ca^{2+} indicator (Rhod-3 AM). As shown in Figure 3, after 808 nm light irradiation for 2 h, the increased fluorescence in the zebrafish that had been treated with DBCO/Cy5.5-UCNs could be observed, while little fluorescence change could be found in zebrafish that had been incubated with PAA/Cy5.5-UCNs but had no DBCO on the cell surface. This clearly suggests that the localized DBCO/

Cy5.5-UCNs labeling could effectively manipulate ion-channel activities in living animals after NIR light illumination. Furthermore, western blot analysis also demonstrated that such NIR-light-gated Ca^{2+} influx in DBCO/Cy5.5-UCNs-incubated zebrafish could lead to the enhanced expression of caspase-3, one key executioner enzyme in cell apoptosis (Figure S16), indicating the feasibility of NIR-light-mediated activation of ion channels to manipulate apoptosis in living animals. Additionally, we also used 4 mm thick pork adipose tissue to further investigate the difference in penetration of 808 nm and 480 nm light irradiation. As expected, the presence of tissue significantly blocks the fluorescence of the Ca^{2+} indicator upon illumination at 480 nm, while the obvious fluorescence could still be found when the tissue was excited at 808 nm (Figure S17), clearly showing that NIR light irradiation could penetrate more deeply to activate the ChR2 channel than the excitation in the conventional visible region. This makes our UCNs-based metabolic strategy suitable for the effective regulation of physiological activities in living systems.

In summary, we introduced a novel and simple strategy based on the native metabolic glyco-biosynthesis to achieve site-specific covalent localization of NIR-light-responsive UCNs on the cell surface through a copper-free click reaction under living conditions. Upon 808 nm light irradiation, the blue emission (at 480 nm) from UCNs could remotely activate the photosensitive ion channel (ChR2) and effectively manipulate the cation influx in living cells and zebrafish. The present strategy not only provides a site-specific and effective approach for the covalently labeling of nanoparticles on the cell membrane, it also holds great potential to precisely regulate the membrane-associated activities under in vivo conditions. Thus, these nanoparticles could act as personalized nanomedicines for various pathological disorders in the future.

Conflict of interest

The authors declare no conflict of interest.

[1] a) L. Fenno, O. Yizhar, K. Deisseroth, *Annu. Rev. Neurosci.* **2011**, *34*, 389–412; b) T. J. Jentsch, C. A. Hübner, J. C. Fuhrmann, *Nat. Cell Biol.* **2004**, *6*, 1039–1047; c) T. Fehrentz, M.

Schönberger, D. Trauner, *Angew. Chem. Int. Ed.* **2011**, *50*, 12156–12182; *Angew. Chem.* **2011**, *123*, 12362–12390.

[2] a) K. Zhang, B. Cui, *Trends Biotechnol.* **2015**, *33*, 92–100; b) M. Banghart, K. Borges, E. Isacoff, D. Trauner, R. H. Kramer, *Nat. Neurosci.* **2004**, *7*, 1381–1386.

[3] a) J. Lin, P. M. Knutsen, A. Muller, D. Kleinfeld, R. Y. Tsien, *Nat. Neurosci.* **2013**, *16*, 1499–1508; b) H. Kobayashi, M. Ogawa, R. Alford, P. L. Choyke, Y. Urano, *Chem. Rev.* **2010**, *110*, 2620–2640.

[4] a) H. Peng, D. T. Chiu, *Chem. Soc. Rev.* **2015**, *44*, 4699–4722; b) E. Papagiakoumou, F. Anselmi, A. Bègue, V. de Sars, J. Glückstad, E. Y. Isacoff, V. Emiliani, *Nat. Methods* **2010**, *7*, 848–854.

[5] a) L. He, Y. Zhang, G. Ma, P. Tan, Z. Li, S. Zang, X. Wu, J. Jing, S. Fang, L. Zhou, Y. Wang, Y. Huang, P. G. Hogan, G. Han, Y. Zhou, *eLife* **2015**, *4*, e10024; b) X. Wu, Y. Zhang, K. Takle, O. Bilsel, Z. Li, H. Lee, Z. Zhang, D. Li, W. Fan, C. Duan, E. M. Chan, C. Lois, Y. Xiang, G. Han, *ACS Nano* **2016**, *10*, 1060–1066; c) S. Shah, J. Liu, N. Pasquale, J. Lai, H. McGowan, Z. P. Pang, K. B. Lee, *Nanoscale* **2015**, *7*, 16571–16577; d) S. Hososhima, H. Yuasa, T. Ishizuka, M. R. Hoque, T. Yamashita, A. Yamanaka, E. Sugano, H. Tomita, H. Yawo, *Sci. Rep.* **2015**, *5*, 16533–16542; e) A. Bansal, H. Liu, M. K. G. Jayakumar, S. Andersson-Engels, Y. Zhang, *Small* **2016**, *12*, 1732–1743.

[6] a) Y. Lu, J. Zhao, R. Zhang, Y. Liu, D. Liu, E. M. Goldys, X. Yang, P. Xi, A. Sunna, J. Lu, Y. Shi, R. C. Leif, Y. Huo, J. Shen, J. A. Piper, J. P. Robinson, D. Jin, *Nat. Photonics* **2014**, *8*, 32–36; b) F. Wang, R. Deng, J. Wang, Q. Wang, Y. Han, H. Zhu, X. Chen, X. Liu, *Nat. Mater.* **2011**, *10*, 968–973; c) W. Fan, W. Bu, J. Shi, *Adv. Mater.* **2016**, *28*, 3987–4011; d) G. Chen, H. Qiu, P. N. Prasad, X. Chen, *Chem. Rev.* **2014**, *114*, 5161–5214; e) X. Zhu, W. Feng, J. Chang, Y. Tan, J. Li, M. Chen, Y. Sun, F. Li, *Nat. Commun.* **2016**, *7*, 10437–10446; f) W. Li, J. Wang, J. Ren, X. Qu, *J. Am. Chem. Soc.* **2014**, *136*, 2248–2251; g) Y. Yang, Q. Shao, R. Deng, C. Wang, X. Teng, K. Cheng, Z. Cheng, L. Huang, Z. Liu, X. Liu, B. Xing, *Angew. Chem. Int. Ed.* **2012**, *51*, 3125–3129; *Angew. Chem.* **2012**, *124*, 3179–3183; h) Y. Min, J. Li, F. Liu, E. K. Yeow, B. Xing, *Angew. Chem. Int. Ed.* **2014**, *53*, 1012–1016; *Angew. Chem.* **2014**, *126*, 1030–1034; i) L. Li, R. Zhang, L. Yin, K. Zheng, W. Qin, P. R. Selvin, Y. Lu, *Angew. Chem. Int. Ed.* **2012**, *51*, 6121–6125; *Angew. Chem.* **2012**, *124*, 6225–6229; j) C. Wang, L. Cheng, Z. Liu, *Theranostics* **2013**, *3*, 317–330.

[7] a) E. M. Sletten, C. R. Bertozzi, *Acc. Chem. Res.* **2011**, *44*, 666–676; b) S. G. Sampathkumar, A. V. Li, M. B. Jones, Z. Sun, K. J. Yarema, *Nat. Chem. Biol.* **2006**, *2*, 149–152; c) N. K. Devaraj, R.

Weissleder, *Acc. Chem. Res.* **2011**, *44*, 816–827; d) Z. Hao, S. Hong, X. Chen, P. R. Chen, *Acc. Chem. Res.* **2011**, *44*, 742–751; e) Y. Zhu, J. Wu, X. Chen, *Angew. Chem. Int. Ed.* **2016**, *55*, 9301–9305; *Angew. Chem.* **2016**, *128*, 9447–9451; f) H. Jiang, B. P. English, R. B. Hazan, P. Wu, B. Ovryn, *Angew. Chem. Int. Ed.* **2015**, *54*, 1765–1769; *Angew. Chem.* **2015**, *127*, 1785–1789; g) R. Xie, L. Dong, Y. Du, Y. Zhu, R. Hua, C. Zhang, X. Chen, *Proc. Natl. Acad. Sci. USA* **2016**, *113*, 5173–5178.

[8] a) D. Yang, Z. Hou, Z. Cheng, C. Li, J. Lin, *Chem. Soc. Rev.* **2015**, *44*, 1416–1448; b) J. Wang, T. Ming, Z. Jin, J. Wang, L. Sun, C. Yan, *Nat. Commun.* **2014**, *5*, 5669–5678; c) W. Zou, C. Visser, J. A. Maduro, M. S. Pshenichnikov, J. C. Hummelen, *Nat. Photonics* **2012**, *6*, 560–564; d) X. Li, F. Zhang, D. Zhao, *Chem. Soc. Rev.* **2015**, *44*, 1346–1378; e) X. Ai, C. J. H. Ho, J. Aw, A. B. E. Attia, J. Mu, Y. Wang, X. Wang, Y. Wang, X. Liu, H. Chen, M. Gao, X. Chen, E. K. L. Yeow, G. Liu, M. Olivo, B. Xing, *Nat. Commun.* **2016**, *7*, 10432–10440; f) W. Zheng, P. Huang, D. Tu, E. Ma, H. Zhu, X. Chen, *Chem. Soc. Rev.* **2015**, *44*, 1379–1415; g) Y. Liu, D. Tu, H. Zhu, R. Li, W. Luo, X. Chen, *Adv. Mater.* **2010**, *22*, 3266–3271; h) S. Lu, D. Tu, P. Hu, J. Xu, R. Li, M. Wang, Z. Chen, M. Huang, X. Chen, *Angew. Chem. Int. Ed.* **2015**, *54*, 7915–7919; *Angew. Chem.* **2015**, *127*, 8026–8030.

[9] a) J. Li, P. R. Chen, *Nat. Chem. Biol.* **2016**, *12*, 129–137; b) Y. Takaoka, A. Ojida, I. Hamachi, *Angew. Chem. Int. Ed.* **2013**, *52*, 4088–4106; *Angew. Chem.* **2013**, *125*, 4182–4200; c) H. Koo, S. Lee, J. H. Na, S. H. Kim, S. K. Hahn, K. Choi, I. C. Kwon, S. Y. Jeong, K. Kim, *Angew. Chem. Int. Ed.* **2012**, *51*, 11836–11840; *Angew. Chem.* **2012**, *124*, 12006–12010.

[10] G. Nagel, T. Szellas, W. Huhn, S. Kateriya, N. Adeishvili, P. Berthold, D. Ollig, P. Hegemann, E. Bamberg, *Proc. Natl. Acad. Sci. USA* **2003**, *100*, 13940–13945.

[11] a) B. Ravikumar, K. Moreau, L. Jahreiss, C. Puri, D. C. Rubinsztein, *Nat. Cell Biol.* **2010**, *12*, 747–757; b) Y. Gao, J. Shi, D. Yuan, B. Xu, *Nat. Commun.* **2012**, *3*, 1033–1040.

[12] S. A. Park, S. Lee, L. Tung, D. T. Yue, *Sci. Rep.* **2014**, *4*, 6125–6135.

[13] S. Orrenius, B. Zhivotovsky, P. Nicotera, *Nat. Rev. Mol. Cell Biol.* **2003**, *4*, 552–565.

[14] R. White, K. Rose, L. Zon, *Nat. Rev. Cancer* **2013**, *13*, 624–636.